Molecular Biology of the Cell
Vol. 21, 3518–3528, October 15, 2010

MAP1B Regulates Axonal Development by Modulating Rho-GTPase Rac1 Activity

Carolina Montenegro-Venegas,*† Elena Tortosa,†‡ Silvana Rosso,§ Diego Peretti,§ Flavia Bollati,§ Mariano Bisbal,§ Ignacio Jausoro,§ Jesus Avila,‡ Alfredo Cáceres,‡ and Christian Gonzalez-Billault*

*Laboratory of Neuronal and Cell Dynamics, Department of Biology, Universidad de Chile and Institute for Cell Dynamics and Biotechnology (ICDB), 7800024 Santiago, Chile; ‡Centro Biología Molecular "Severo Ochoa" Cantoblanco, 28049 Madrid, CSIC-UAM, Spain; and §Instituto Mercedes y Martín Ferreyra (INIMEC-CONICET), 5000 Córdoba, Argentina

Submitted August 19, 2009; Revised July 28, 2010; Accepted August 9, 2010
Monitoring Editor: Erika Holzbaur

Cultured neurons obtained from MAP1B-deficient mice have a delay in axon outgrowth and a reduced rate of axonal elongation compared with neurons from wild-type mice. Here we show that MAP1B deficiency results in a significant decrease in Rac1 and cdc42 activity and a significant increase in Rho activity. We found that MAP1B interacted with Tiam1, a guanosine nucleotide exchange factor for Rac1. The decrease in Rac1/cdc42 activity was paralleled by decreases in the phosphorylation of the downstream effectors of these proteins, such as LIMK-1 and cofilin. The expression of a constitutively active form of Rac1, cdc42, or Tiam1 rescued the axon growth defect of MAP1B-deficient neurons. Taken together, these observations define a new and crucial function of MAP1B that we show to be required for efficient cross-talk between microtubules and the actin cytoskeleton during neuronal polarization.

INTRODUCTION

Neurons are highly polarized cells that contain a single long axon and several dendrites. Polarization occurs when one of the multiple neurites emerging from the cell body initiates a phase of rapid elongation, becoming an axon. Axon formation is causally related to dramatic changes in the organization and dynamics of the growth cone cytoskeleton. These changes involve an expansion of the peripheral lamellipodial veil, a shortening of actin ribs, an increase in actin dynamics, and the penetration of tyrosinated (presumably dynamic) microtubules within the central growth cone region (Bradke and Dotti, 1997, 1999; Kunda *et al.*, 2001). In the presence of the actin-depolymerizing drug, cytochalasin D, all minor processes can generate an axon. This treatment leads to multiple axon formation, a phenomenon preceded by the penetration of microtubules within neuritic tips devoid of actin filaments (Bradke and Dotti, 1999; Ruthel and Hollenbeck, 2000; Kunda *et al.*, 2001). Therefore, if all neurites have the potential to become an axon, what causes cytoskeletal changes at one particular neuritic growth cone so that this neurite but none of the others becomes the axon? This process has been proposed to depend on a polarity complex that includes microtubule-modifying proteins such as crmp2 and molecules that regulate actin polymerization, such as cdc42 (Inagaki *et al.*, 2001; Nishimura *et al.*, 2005; Sosa *et al.*, 2006). A reasonable hypothesis is that axon formation takes place from the growth cone that has a more dynamic microtubule polymer, which promotes lamellipodial protrusion and expansion similar to what occurs in migrating fibroblasts (Waterman-Storer *et al.*, 1999). Moreover, it has been also described the importance of local microtubule stabilization to induce axon formation (Witte *et al.*, 2008).

To test this hypothesis, we have focused our attention on the microtubule-associated protein MAP1B. There are several reasons for this choice. MAP1B is the first MAP that is expressed and is especially prominent in developing neurons, being highly concentrated at the distal tip of growing axons where it associates with tyrosinated microtubules (Black *et al.*, 1994). Suppression of MAP1B with antisense oligonucleotides inhibits laminin-enhanced axonal growth (DiTella *et al.*, 1996). Furthermore, targeted disruption of the MAP1B gene results in an impairment of brain development (Edelmann *et al.*, 1996; Takei *et al.*, 1997; Gonzalez-Billault *et al.*, 2000; Meixner *et al.*, 2000; Takei *et al.*, 2000), altering processes that are dependent on the appearance of neuronal cytoplasmic extensions such as neuronal migration (Gonzalez-Billault *et al.*, 2005) and axonal guidance (Del Rio *et al.*, 2004). More importantly, cultured hippocampal pyramidal neurons obtained from MAP1B-deficient mice have a significant delay in axon outgrowth and a reduced rate of axonal elongation (Takei *et al.*, 2000; Gonzalez-Billault *et al.*, 2001). These neurons display growth cones with small lamellipodial veils, as well as decreased microtubule assembly

This article was published online ahead of print in *MBoC in Press* (http://www.molbiolcell.org/cgi/doi/10.1091/mbc.E09–08–0709) on August 18, 2010.

† These authors contributed equally to this work.

Address correspondence to: Christian Gonzalez-Billault (chrgonza@uchile.cl).

and dynamics that are quite evident at the distal axonal tip, where the more recently assembled microtubule polymer normally predominates (Gonzalez-Billault *et al.*, 2001). MAP1B is not only a microtubule-associated protein but also an actin-binding protein (Pedrotti and Islam, 1996; Cueille *et al.*, 2007). It has been proposed that MAP1B, apart from being a microtubule-stabilizing protein, may also function as a scaffold protein (Riederer, 2007). In this work, we show that MAP1B participate in the regulation of the cross-talk between microtubules and actin microfilaments to facilitate axonal development.

MATERIALS AND METHODS

Cell Culture

Cultures of dissociated hippocampal pyramidal cells from wild-type (WT) and MAP1B knockout mouse embryonic brain tissue were prepared as described (Gonzalez-Billault *et al.*, 2001). All cultures were maintained in a humidified 37°C incubator with 5% CO_2. For some experiments, cytochalasin D was added to the cultures at a concentration of 0.5 μg/ml for 3, 6, and 12 h.

Expression Plasmids and Transfection

The following plasmids were used for transfection of primary cultures: 1) Tiam1 cDNA (C1199; Kunda *et al.*, 2001) cloned as a BamHI/XhoI fragment into pcDNA3 containing a cytomegalovirus promoter and a hemagglutinin tag; 2) cDNA for constitutively active Rac1 (CA-Rac1, V12 mutant) and another for WT-Rac1 cloned in pcDNA3 containing a myc tag; and 3) A cDNA for WT cdc42 and another for constitutively active cdc42 (V12 cdc42) cloned in pcDNA3 containing a myc tag. Transient transfection of cultured neurons was performed using the Amaxa mouse neuron nucleofector kit (Gaithersburg, MD). The neurons were nucleofected at 0 DIV (days in vitro), and all cDNAs were used at concentrations of 3 μg/ml. Cells were analyzed 24 h after transfection.

Primary Antibodies

The following primary antibodies were used in this study: anti-tyrosinated α-tubulin mAb (clone TUB-1A2, mouse IgG, Sigma Chemical Co., St. Louis, MO) diluted 1:2000; anti-α-tubulin mAb (Sigma) diluted 1:2000; a goat Ab against MAP1B diluted 1:2000 (N-19, Santa Cruz Biotechnology, Santa Cruz, CA); rabbit antibody against Tiam1 diluted 1:200 (Santa Cruz Biotechnology); anti-hemagglutinin mAb diluted 1:1000; a mAb against myc diluted 1:500 (Santa Cruz Biotechnology); goat antibody against p-MYPT1 diluted 1:500 (Santa Cruz Biotechnology); anti-cofilin mAb diluted 1:1000, a generous gift of Dr. James Bamburg (Colorado State University); rabbit antibody against P-cofilin diluted 1:1000, a gift of Dr. Bamburg; goat antibody against Limk-1 (Santa Cruz Biotechnology) diluted 1:1000; rabbit antibody against P-Limk1 diluted 1.1000 (Cell Signaling, Beverly, MA), phalloidin-TRITC (Sigma) and phalloidin-FITC (Molecular Probes, Eugene, OR) to label the actin cytoskeleton diluted 1:200. Antibodies against Rac1, Cdc42, and RhoA (Cytoskeleton, Denver, CO) diluted 1:500.

Immunofluorescence

Cells were fixed before or after detergent extraction under microtubule-stabilizing conditions and processed for immunofluorescence as described (Kunda *et al.*, 2001). For some experiments, in order to visualize the association of Rac1 with the growth cone cytoskeleton, cells were fixed as described by Nakata and Hirokawa (Nakata and Hirokawa, 1987; Paglini *et al.*, 1998). The antibody staining protocol was carried out as described (Kunda *et al.*, 2001). Cells were analyzed in a Zeiss LSM 410 confocal scanning microscope or in an inverted microscope (Zeiss Axiovert 35M) equipped with epifluorescence and differential interference contrast optics (Thornwood, NY). The relative intensities of Rac1, Tiam1, and F-actin staining were evaluated in fixed unextracted cells or in detergent-extracted cytoskeletons using quantitative fluorescence techniques as described (Paglini *et al.*, 1998). Images were collected using a CCD camera (Orca 1000) and Metamorph software. To measure axonal length, cells were analyzed with a Zeiss LSM 510 META confocal scanning microscope.

Immunoprecipitation

The cortex and hippocampus of a mouse brain collected on embryonic day 18 (E18) were homogenized in 0.7 ml of cold immunoprecipitation buffer (1% wt/vol Triton X-100, 150 mM NaCl, 10 mM Tris, pH 7.4, 1 mM EDTA, 1 mM EGTA, pH 8.0, 0.2 mM sodium orthovanadate, 0.2 mM phenylmethylsulfonylfluoride [PMSF], and 0.5% wt/vol Nonidet P40). The homogenate was centrifuged at 16,000 $\times$ *g* for 15 min at 4°C, and the supernatant was collected as the total cell lysate.

To 400 μg of the supernatant, 5 μg of a specific antibody was added in a final volume of 1 ml. The solution was mixed with a vortex and incubated for another 1 h at 4°C. Then 20 μl of 50% protein A-agarose bead solution was added, mixed, and incubated with agitation for 30 min at 4°C. The beads were pelleted by centrifugation at 16,000 $\times$ *g* for 15 min at 4°C, and the supernatant was removed. The pellet was washed twice with immunoprecipitation buffer and resuspended in 30 μl of twofold-concentrated electrophoresis sample buffer (250 mM Tris, pH 6.8, 4% [wt/vol] SDS, 10% glycerol, 0.006% bromophenol blue, and 2% [wt/vol] 2-mercaptoethanol). The proteins were separated by gel electrophoresis, and the fractionated proteins were then characterized by Western blot analysis.

Rho-GTPase Activity Assays and Western Blotting

The Rac1 activity assay was done essentially as described (Waterman-Storer *et al.*, 1999). Briefly, cultures of hippocampal pyramidal neurons (1 DIV) were lysed at 4°C in 50 mM Tris, 150 mM NaCl, 1% Triton X-100, and 0.5% deoxycholate, pH 7.2. GTP-bound Rac1 was affinity-precipitated from cell lysates at 4°C by using an immobilized GST fusion of the Rac1-binding domain of murine PAK, which binds Rac1-GTP but not Rac1-GDP. Bound proteins were separated by 12% SDS-PAGE and Western-blotted with anti-Rac1 (Rac1 activation assay Biochem kit; Cytoskeleton). Pulldown assays of activated cdc42 were carried out as described for Rac1, but were probed with an antibody against cdc42 (Cytoskeleton,). Pulldown assays and western blotting for activated RhoA were performed as described for Rac1, but using an immobilized GST fusion of the Rho binding domain of the Rho effector protein, rhotekin. The Rho binding domain motif has been shown to bind specifically to the GTP-bound form of RhoA. Total RhoA and RhoA-GTP were detected with mouse anti-RhoA mAbs (RhoA activation assay; Biochem kit; Cytoskeleton).

Protein Extracts and Western Blots

Protein extracts were prepared from hippocampal pyramidal neuron cultures and from the cortex and hippocampus of an embryonic mouse brain (E18) in 20 mM HEPES, pH 7.4, containing 0.1 mM NaCl, 10 mM NaF, 1 mM Na_3VO_4, 5 mM EDTA, 1 mM okadaic acid, and protease inhibitors (2 mM PMSF, 10 mg/ml aprotinin, 10 mg/ml leupeptin, 10 mg/ml pepstatin). Protein samples were separated by SDS-PAGE, electroblotted onto nitrocellulose sheets, developed with an ECL chemiluminescence system, and quantified by densitometry.

Morphometric Analysis of Neuronal Shape Parameters

Images were digitized on a video monitor using Metamorph software (Universal Imaging, West Chester, PA). To measure neurite length or growth cone shape parameters, antibody-labeled cells were randomly selected and traced from a video screen using the morphometric menu of Metamorph software as described (Paglini *et al.*, 1998; Kunda *et al.*, 2001). Axonal lengths were measured using the ImageJ program (http://rsb.info.nih.gov/ij/). Differences among groups were analyzed using ANOVA and the Student-Newman-Keuls test.

RESULTS

The Delay in Axonal Development in Map1B−/− Neurons Is Related to a Defect in the Actin Cytoskeleton

To investigate whether MAP1B promotes axon formation by regulating growth cone lamellipodial expansion and hence actin dynamics, we first analyzed the response of MAP1B-deficient (−/−) neurons to treatment with cytochalasin D, an inhibitor of actin polymerization. Our aim was to determine whether the inhibition of axon formation observed in MAP1B-deficient neurons was primarily related to decreased microtubule assembly, as originally postulated (Gonzalez-Billault *et al.*, 2001), or to a failure to induce a highly dynamic actin cytoskeleton permissive for microtubule assembly, invasion, and subsequent growth. Figure 1, A and B, are representative confocal images of pyramidal neurons from MAP1B+/+ and MAP1B−/− mice, respectively, treated with antibodies against α-tubulin (green) and rhodamine-phalloidin (red). Briefly, MAP1B-deficient neurons displayed shorter axons when compared with control neurons, consistent with previously reported results (Gonzalez-Billault *et al.*, 2001). To analyze the role of local actin polymerization, we treated control and MA1B−/− cells with cytochalasin D. As reported (Bradke and Dotti, 1999), WT cultured hippocampal pyramidal neurons treated

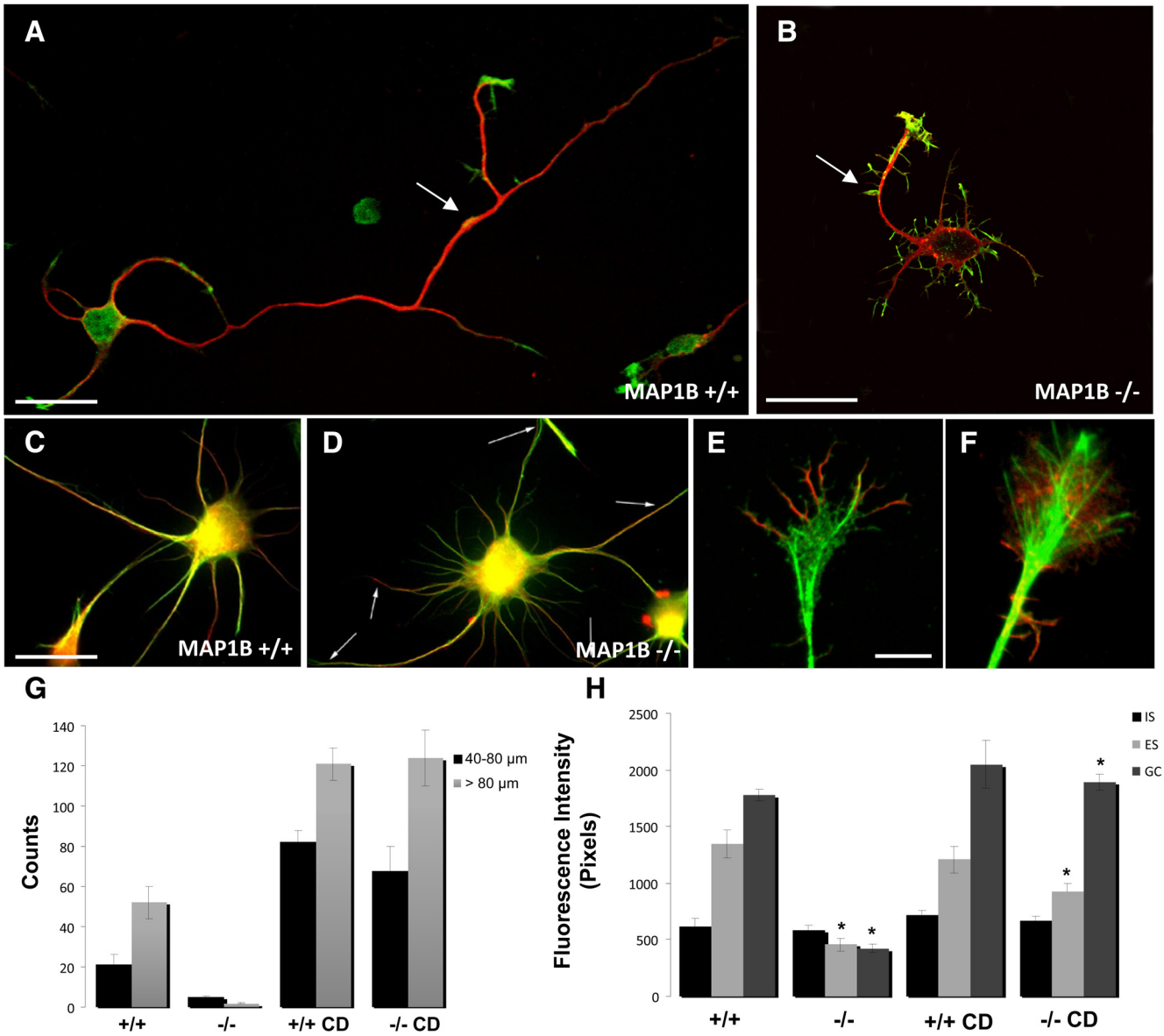

Figure 1. Cytochalasin D restores the kinetics of axon development in MAP1B-deficient cells. Cytochalasin D induced multiple axon formation and promoted microtubule assembly in MAP1B-deficient neurons. (A) Morphology and distribution of α-tubulin (red) and rhodamine-phalloidin (green) in WT hippocampal pyramidal neurons and in MAP1B-deficient neurons. (B) Whereas WT-neurons extended a single long axon under control conditions (A), MAP1B-deficient neurons failed to do so. However, both WT and MAP1B-deficient neurons were capable of extending multiple axon-like neurites after treatment with cytochalasin D (0.5 μg/ml). (C and D) Morphology of WT neurons and MAP1B$-/-$ neurons, respectively, after 6 h of treatment with cytochalasin D, shown as a red (Glu-tubulin) and green (Tyr-tubulin) overlay. (E) Morphology of the growth cone from a WT neuron in the absence of cytochalasin D shown as a red (F-actin) and green (Tyr-tubulin) overlay. (F) Same conditions as in E after 3 h of treatment of WT neurons with cytochalasin D. The treatment induced the penetration of Tyr-microtubules within areas devoid of actin filaments. Note that microtubules reach the outer rim of the flattened neuritic tip. (G) Graph showing the number of neurites extending for more than 40 μm in untreated or cytochalasin D–treated neuronal cultures obtained from WT ($+/+$) or MAP1B-deficient ($-/-$) neurons. (H) Quantitative fluorescent measurements of tyrosinated tubulin immunolabeling in cytoskeletal preparations from untreated and cytochalasin D–treated hippocampal pyramidal neurons of WT and MAP1B-deficient neurons. Measurements were performed in the initial segment (IS), external segment (ES), and growth cone (GC) of axons of WT neurons or of the longest neurite of untreated MAP1B-deficient neurons. In the case of cytochalasin D–treated neurons, measurements were performed in all neurites extending more than 80 μm. A total of 50 cells were analyzed for each experimental condition. Cells were treated with cytochalasin D (0.5 μg/ml) for 12 h. All cultures were fixed for 36 h after plating. Bar, 10 μm.

for a short period with low doses of cytochalasin D extend multiple long axon-like neurites (Figure 1C). Interestingly, an identical phenomenon was observed in MAP1B-deficient neurons (Figure 1D). Double immunofluorescence visualization of cytochalasin D–treated MAP1B$+/+$ neurons with antibodies against tyrosinated (Tyr-tub) and detyrosinated (Glu-tub) α-tubulin clearly revealed the presence of many dynamic microtubules at neuritic tips (Figure 1F). Quantitative fluorescence measurements revealed that cytochalasin D increased the Tyr-tubulin staining of axon-like neurites, an effect that selectively occurred at the distal end of growing processes. Furthermore, in the presence of cytochalasin

D, no differences in Tyr-tubulin staining were detected between WT and MAP1B-deficient neurons (Figure 1G). Taken together, these results demonstrate that after cytochalasin D treatment, MAP1B-deficient neurons were not only able to generate axon-like neurites but also as capable as WT neurons at assembling microtubules. Theses results suggest that there was not a general defect in cytoskeleton components in MAP1B−/− mice but rather a defect in the regulation of the assembly of their components.

MAP1B Deficiency Modifies Activities of the Rho-GTPases Rac1 and Cdc42

It follows that one primary function of MAP1B during initial axon outgrowth may also be related to the regulation of actin organization and the promotion of microtubule assembly. To test this possibility, we examined whether MAP1B deficiency altered the levels and/or activity of Rac1 or cdc42. Rac1 and cdc42 are two small Rho-GTPases that are involved in lamellipodial and filopodial expansion/protrusion, respectively (Bishop and Hall, 2000) and are required for axon outgrowth, elongation, and branching (Luo, 2000, 2002; Ng *et al.*, 2002). These proteins act as a molecular switch cycling between an active GTP-bound and inactive GDP-bound state. First, we determined that Rac1 was highly expressed in growth cones of embryonic brain tissue (data not shown). Next, to determine whether MAP1B was involved in the regulation of Rac1 activity, we measured the amount of GTP-bound Rac1 in cultured neurons derived from WT and MAP1B-deficient mice after 1 DIV. To measure Rac1 activity, we used a glutathione *S*-transferase (GST) fusion protein corresponding to the p21-binding domain (residues 67–150) of murine PAK1, a Rac effector that binds with high-affinity to Rac1-GTP but not Rac1-GDP in a pull-down assay. We found that cell extracts from MAP1B-deficient mice had significantly lower Rac1 activity than extracts from WT mice (Figure 2A). Total Rac1 protein levels were similar in MAP1B-deficient neuron extracts and control samples (Figure 2A). Quantitative analyses showed that there was a 90% decrease in Rac1 activity in MAP1B-deficienct neurons compared with control neurons (Figure 2A, right). Next, we analyzed whether the overexpression of CA-Rac or WT-Rac could induce axon formation in MAP1B−/− neurons. Overexpression of CA-Rac1 in transfected MAP1B-deficient neurons resulted in extensions that resembled axon-like neurites (Figure 2, B and D). These neurites displayed growth cones with prominent lamellipodial veils, as well as growth cone-like structures located along the main axonal shaft, which are two features of rapidly growing axons (Bradke and Dotti, 1999; Ruthel and Banker, 1999). In contrast, overexpression of WT-Rac1 in transfected MAP1B-deficient neurons had no effect on promoting axon extension (Figure 2, B and C). Quantitative analyses revealed that the MAP1B-deficient neurons trans-

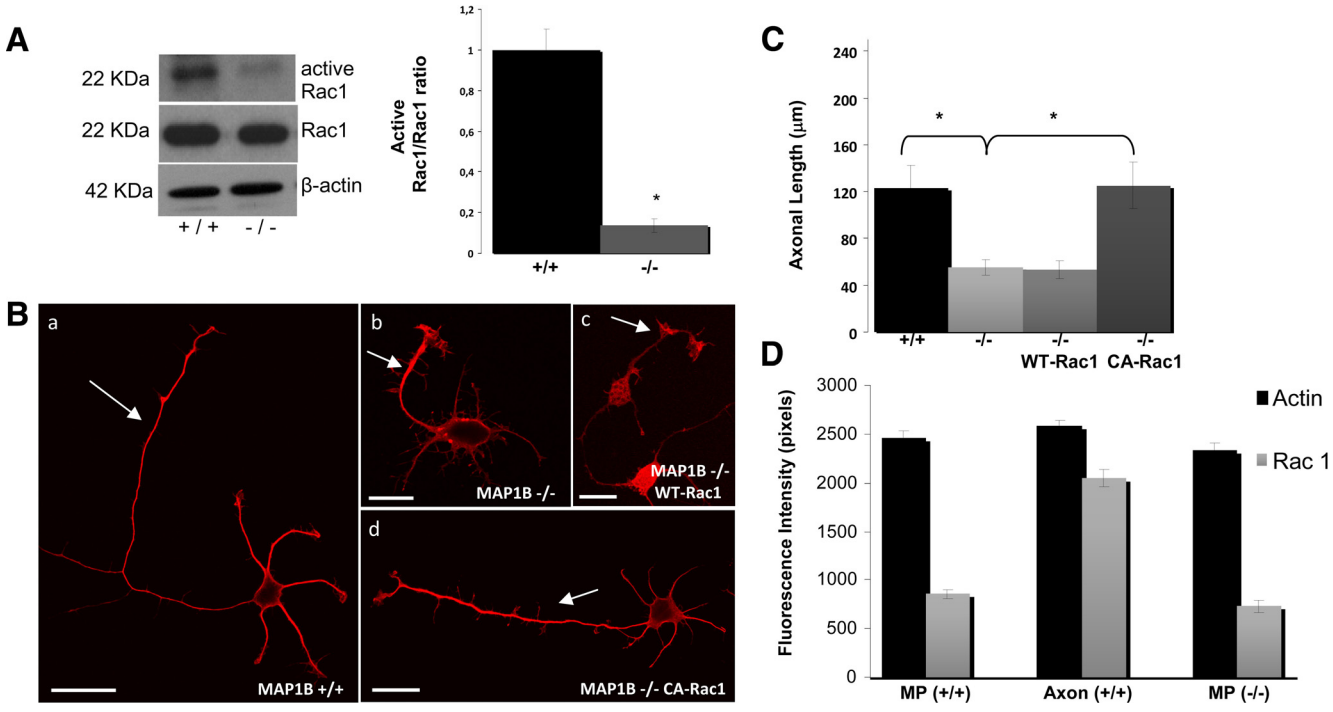

Figure 2. MAP1B deficiency decreases Rac1 activity. (A) Western blot showing that neuron culture extracts obtained from the embryonic hippocampus of WT (+/+) mice contain considerably more Rac1-GTP than equivalent samples obtained from MAP1B-deficient (−/−) animals. Total Rac1 and β-actin were used as loading control. Quantitative analysis confirmed a significant decrease (*$p \leq 0.05$) in Rac1 activity in MAP1B-deficient cells. (B) Morphology of a hippocampal MAP1B (+/+) neuron as shown by confocal microscopy (a). The cell displays one single long axon and was stained with an antibody against α-tubulin (red). Morphology of a hippocampal MAP1B (−/−) neuron as shown by confocal microscopy (b). The cell displays a very short axon-like neurite and was stained as in panel a. The short axon-like neurite in a MAP1B (−/−) neuron transfected with Rac1-WT resembles neurites in MAP1B (−/−) neurons. Morphology of a MAP1B-deficient neuron transfected with myc-tagged constitutively active Rac1 (CA-Rac1) after plating and then fixing 24 h later; cells were visualized by confocal microscopy. Cells were stained with an antibody against c-myc. Note that the cell displays a long axon-like neurite and several much shorter minor neurites. Bars, 10 μm. (C) Quantitative analyses indicated that MAP1B-deficient neurons transfected with CA-Rac1 displayed axons with a length similar to WT neurons (*$p \leq 0.05$). (D) Quantitative fluorescence measurements of Rac1 and phalloidin immunolabeling in cytoskeletal preparations from WT (+/+) and MAP1B-deficient (−/−) cultured hippocampal pyramidal neurons. Measurements were performed within a 10-μm area located at the periphery of growth cones of minor processes and axons.

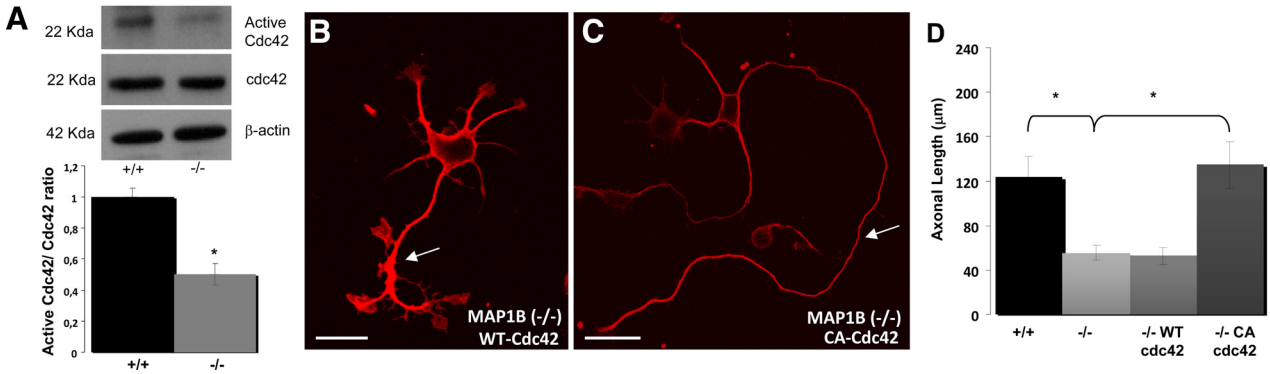

Figure 3. MAP1B deficiency decreases cdc42 activity. (A) Western blot showing that neuron culture extracts obtained from the embryonic hippocampus of WT (+/+) mice contain more cdc42-GTP than equivalent samples obtained from MAP1B-deficient (−/−) animals. Total cdc42 and β-actin were used as loading controls. Quantitative analysis confirmed a significant decrease (*p ≤ 0.05) in cdc42 activity in MAP1B-deficient cells. (B) Morphology of a MAP1B-deficient (−/−) neuron transfected with myc-tagged WT-cdc42 after plating and fixing 24 h later, as visualized by confocal microscopy. Cells were stained with an antibody against c-myc. Note that the cell displays a short axon-like neurite similar to those seen in MAP1B-deficient neurons. Bar, 10 μm. (C) Morphology of a MAP1B (−/−) neuron transfected with myc-tagged constitutively active cdc42 (CA-cdc42). Cells were stained as in B. Note that the cell displays a long single axon-like neurite (arrow). Bar, 10 μm. (D) Quantitative analyses indicated that MAP1B-deficient neurons transfected with CA-cdc42 had axons of length similar to WT (+/+). *p ≤ 0.05.

fected with CA-Rac1 extended axons of similar length to that of WT neurons (Figure 2C).

Because activated Rac1 binds to membranes, we used high-resolution fluorescence microscopy and quantitative fluorescence to analyze its subcellular distribution in detergent-extracted cytoskeletal fractions prepared under conditions that stabilize cytoskeletal-membrane interactions (Nakata and Hirokawa, 1987). In WT neurons, the highest immunofluorescence signals for Rac1 were detected in the peripheral lamellipodial veil of axonal growth cones and in the largest unpolarized neurons. Lower immunofluorescence signals were detected in the growth cones of the remaining minor processes (Figure 2D). The intensities of these signals were equivalent to those observed in the growth cones of MAP1B-deficient neurons, either displaying only minor processes or minor processes plus a short axon.

We performed a similar analysis to test whether cdc42 activation was also affected in MAP1B-deficient neurons.

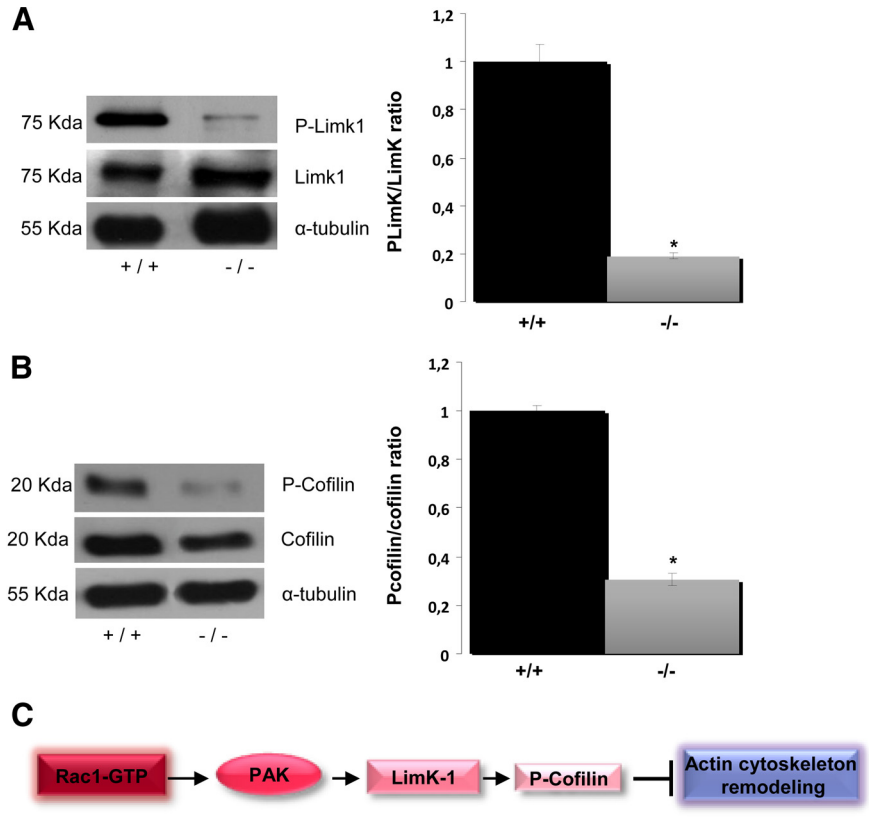

Figure 4. MAP1B deficiency induces changes in the amount of activated proteins downstream of Rac1. (A) Western blots showed diminished levels of phosphorylated LIMK in brain extracts derived from MAP1B (−/−) mice compared with WT (+/+) littermates. Quantitative analyses of the ratio between phosphorylated and nonphosphorylated LIMK are indicated. *p ≤ 0.05. (B) Western blots showing decreased levels of phosphorylated cofilin in brain extracts derived from MAP1B (−/−) mice compared with WT (+/+) littermates. Quantitative analyses indicated the ratio between phosphorylated and nonphosphorylated cofilin was significant; p ≤ 0.05. (C) Schematic showing the downstream effectors of Rac1.

Activation of cdc42 has been proposed to be required for proper Rac1 activation in neuronal cells (Nishimura *et al.*, 2005). As expected, there was a 50% decrease in cdc42 activity in MAP1B-deficient cells compared with control cells (Figure 3A). These changes were independent of the overall amount of cdc42 (Figure 3A). We also determined that overexpression of CA-cdc42 in MAP1B−/− neurons induced axon formation (Figure 3C), whereas overexpression of WT-cdc42 had no significant effect (Figure 3B). Quantitative analyses showed that overexpression of CA-cdc42 in MAP1B−/− cells induced formation of axons with lengths similar to those of WT neurons (Figure 3D).

Decreased Phosphorylation of LIMK-1 and Cofilin in MAP1B-deficient Neurons

The signaling cascade downstream of Rac1 and cdc42 activation involves the activation of the serine/threonine protein kinase LIMK-1 (Arber *et al.*, 1998; Yang *et al.*, 1998). LIMK-1, a downstream effector of Rac1 activity, phosphorylates the actin-binding protein cofilin (Yang *et al.*, 1998). Transitions between the phosphorylated and dephosphorylated forms of cofilin are responsible for changes in the content of actin microfilaments (Bamburg and Bray, 1987; Bamburg, 1999; Sarmiere and Bamburg, 2004). Therefore, we

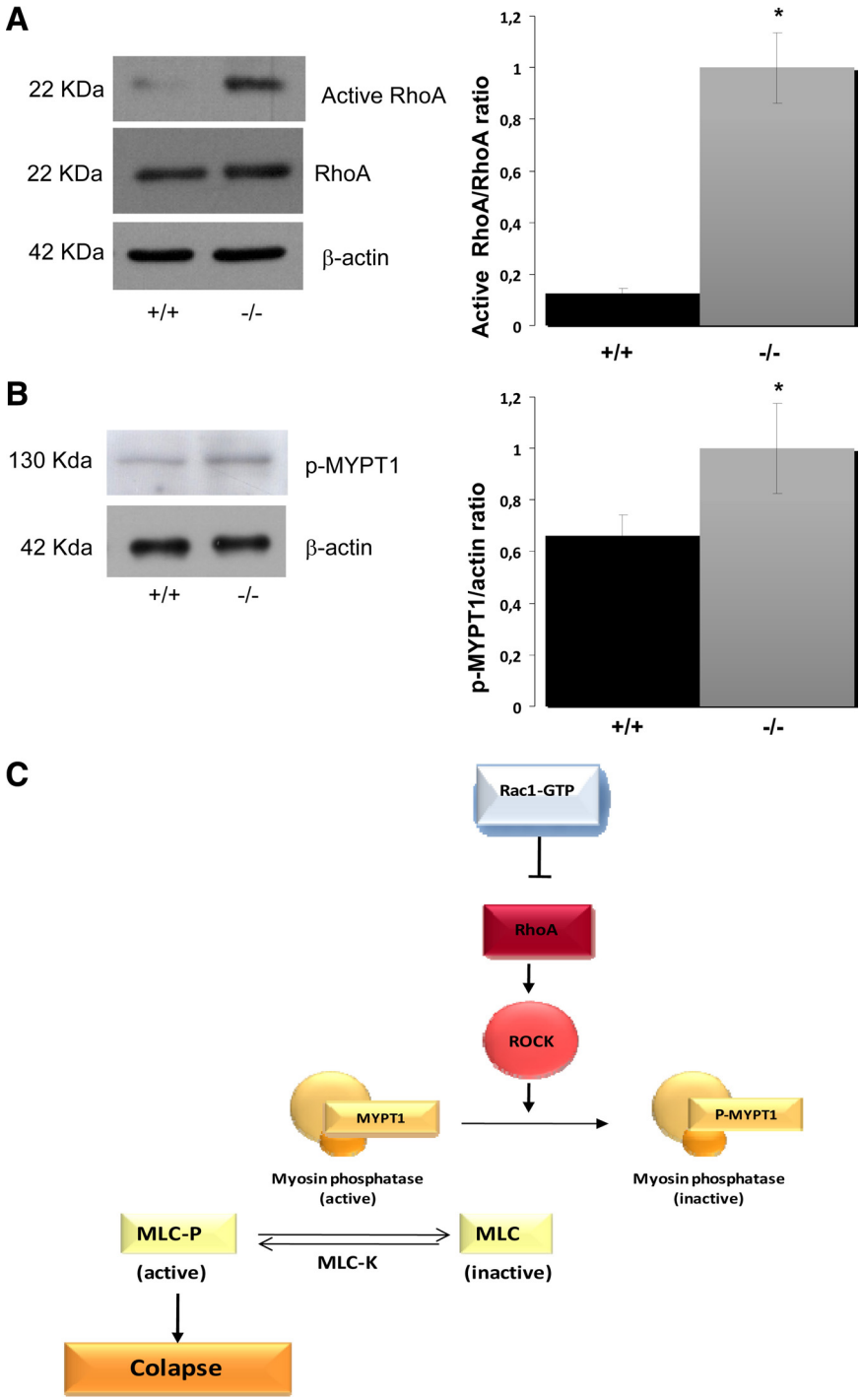

Figure 5. MAP1B deficiency increases RhoA activity. (A) Western blot showing that neuron culture extracts obtained from the embryonic hippocampus of WT (+/+) mice contain considerably less RhoA-GTP than equivalent samples obtained from MAP1B-deficient (−/−) animals. Total RhoA and β-actin were used as loading controls. Quantitative analysis confirmed significantly increased RhoA activity in MAP1B-deficient cells ($p \leq 0.05$). (B) Western blot showing that brain extracts derived from WT (+/+) mice had increased phosphorylation of MYPT1 (p-MYPT1) compared with equivalent samples obtained from MAP1B-deficient animals (−/−). Quantitative analyses confirmed significantly increased phosphorylation of MYPT1 ($p \leq 0.05$). (C) Schematic showing the RhoA pathway in which MYPT1 is involved.

analyzed whether decreased Rac1 activity was associated with changes in the activation of LIMK-1 and cofilin. Phosphorylated LIMK-1 was diminished in protein extracts derived from MAP1B-deficient neurons compared with WT neurons (Figure 4A). The ratio of phospho-LIMK-1 to total LIMK-1 was also significantly decreased in MAP1B-deficient neurons (Figure 4A, right). We then analyzed phosphorylated cofilin levels in protein extracts derived from MAP1B-deficient neurons. Similarly to LIMK-1, phosphorylated cofilin was also decreased in MAP1B-deficient neurons compared with WT neurons (Figure 4B). These results reinforce the hypothesis that MAP1B loss-of-function leads to decreased Rac1 activity and subsequently affects the signaling cascade that controls actin polymerization. Figure 4C shows one of the signaling cascades downstream of Rac1 activation.

Increased RhoA Activity in MAP1B-deficient Neurons

RhoA is a GTPase involved in neurite collapse (Bishop and Hall, 2000), and it has been suggested that Rac1 activation may result in decreased RhoA activity (Da Silva *et al.*, 2003; Ik-Tsen Heng *et al.*, 2009). To test whether the decrease in Rac1 activity observed in MAP1B-deficient neurons could result in increased RhoA activity, we analyzed effects of MAP1B deficiency on RhoA activation. RhoA activity in MAP1B-deficient neurons was increased compared with control WT neurons (Figure 5A). This change was not due to increased RhoA expression because the overall levels of RhoA were similar in WT and MAP1B-deficient neurons (Figure 5A). Quantitative analyses indicated a dramatic 80% increase in RhoA activation in MAP1B-deficient cells (Figure 5A, right). The canonical signaling pathway downstream of RhoA includes activation of the serine/threonine kinase RhoK (Maekawa *et al.*, 1999). Therefore, we assessed the effects of MAP1B deficiency on phosphorylation of MYPT1, a specific substrate for Rho-kinase. Consistently, there was a significant increase in the amount of phospho-MYPT1 in neurons derived from MAP1B-deficient mice compared with WT mice (Figure 5B). Increased phospho-MYPT1 would result in an increased growth cone collapse. Figure 5C shows the RhoA signaling pathway where MYPT1 is involved.

Reduced Interaction of Tiam1 with Rac1 in MAP1B-deficient Neurons

Having shown that MAP1B deficiency was associated with decreased Rac1 activity, we sought to determine the molecular mechanism implicated in Rac1 inactivation. The invasion-inducing T-lymphoma and metastasis 1 protein (Tiam1) functions as a guanine nucleotide exchange factor (GEF) for Rac1 stimulating Rac1 activity (Figure 6A). Tiam1 behaves as a microtubule-associated protein in brain tissues, and it interacts with dynamic microtubules of the axonal growth cone and promotes axon formation in cultured hippocampal neurons (Kunda *et al.*, 2001). We first analyzed the distribution of Tiam1 in WT and MAP1B−/− neurons. In WT neurons, Tiam1 was mainly found at the distal end of axons including the growth cones (Figure 6B). In MAP1B-deficient neurons, most of the staining was located in the cell body (Figure 6C). Because Tiam1 is a GEF for Rac1, we decided to measure the amount of Tiam1 bound to Rac1-GTP in our pulldown assay. We found a dramatic decrease of Tiam1 bound to Rac-GTP in MAP1B-deficient neurons compared with WT (Figure 6F). This change was not dependent on the level of Tiam1 expression because the amounts of Tiam1 and Rac1 in hippocampal cell lysates were similar in WT control and MAP1B-deficient cells (Figure 6F). Quantitative analyses indicated that Tiam1–Rac1–GTP complex formation in MAP1B-deficient neurons was decreased by 70% compared with WT controls (Figure 6F, right).

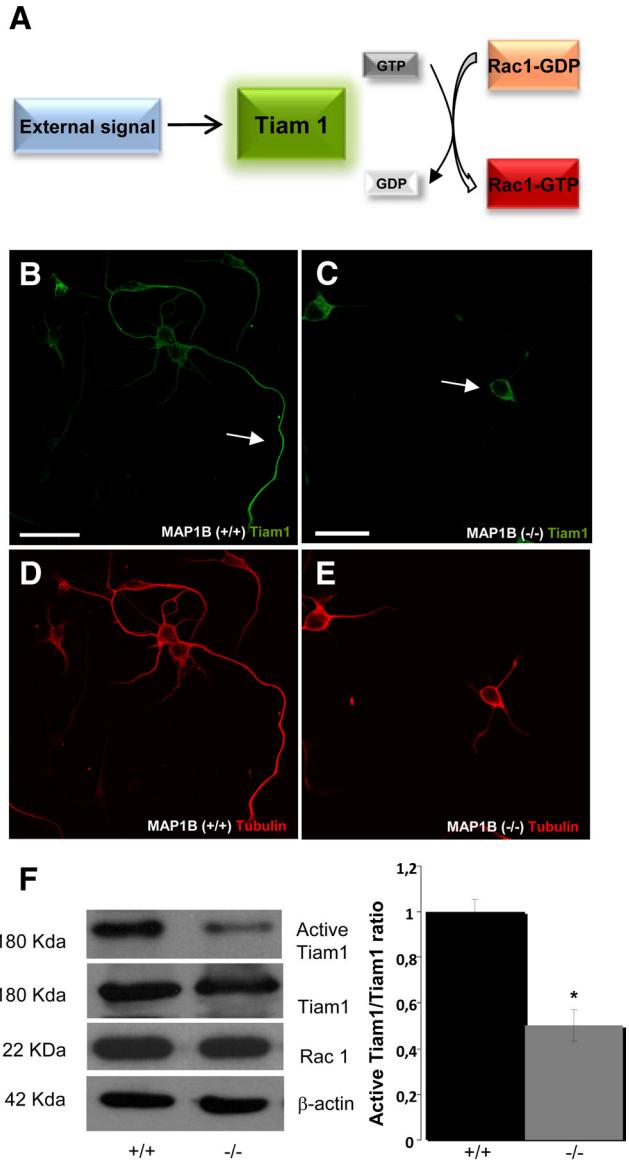

Figure 6. MAP1B deficiency alters Tiam1 distribution and its binding to Rac1. (A) Schematic showing that an external signal activates Tiam1, which facilitates GDP for GTP exchange on Rac1, thereby activating Rac1. (B and C) Representative confocal images from hippocampal WT MAP1B (+/+) and MAP1B-deficient (−/−) neurons, respectively. The cells were stained with anti-Tiam1 (green). Note that the distribution of Tiam1 in MAP1B (+/+) neurons was predominantly in the axon and less in soma. In contrast the distribution in MAP1B−/− was predominantly in the soma. Bar, 10 μm. (D and E) Fluorescence images shown the morphology of WT MAP1B (+/+) and MAP1B (−/−), respectively, inmunostaining with α-tubulin (red). (F) Decreased Tiam1–Rac1 interactions in pulldown assays using supernatants derived from MAP1B-deficient neurons (−/−). These changes were not due to changes in the expression of either Rac1 or Tiam1. β-Actin was used as a loading control. Quantitative analysis confirmed a significant decrease in Tiam1–Rac1 interactions in MAP1B-deficient neurons (*p $\leq$ 0.05).

We then sought to determine whether it was possible to induce axon formation in MAP1B-deficient neurons by overexpressing a Tiam1 variant that localizes to the plasma membrane and is constitutively active (CA-Tiam1; clone

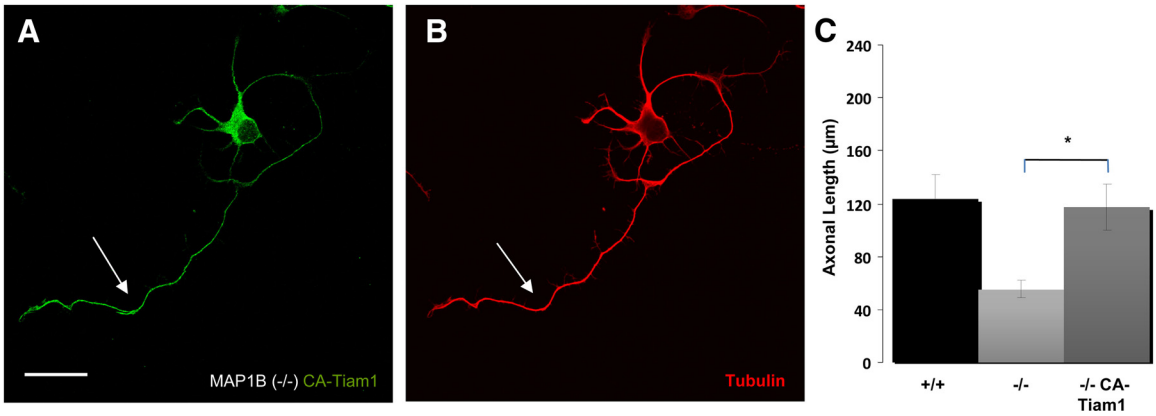

Figure 7. Tiam1 overexpression can rescue the kinetics of axonal elongation in MAP1B-deficient neurons. (A and B) Confocal micrographs showing the morphology of a MAP1B-deficient neuron (−/−) transfected with C1199 (CA-Tiam1), a constitutively active variant that can efficiently activate Rac1. The neurons were transfected after plating and then were fixed 24 h later and stained with anti-Tiam1 and a mAb against tyrosinated α-tubulin. Note that the cell developed a single long axon-like neurite (arrow in each panel). Bar, 10 μm. (C) Quantitative analyses indicated that the MAP1B-deficient neurons transfected with CA-Tiam1 displayed axons with a length similar to WT (+/+) neurons (*$p \leq 0.05$).

C1199; Kunda *et al.*, 2001). Expression of CA-Tiam1 rescued the axon growth defect in MAP1B-deficient neurons (Figure 7, A and B). Reversal of the axonal elongation defect in MAP1B−/− neurons via overexpression of CA-Tiam1 was statistically significant (Figure 7C).

Tiam1 Interacts with MAP1B

Finally, we tested whether MAP1B binds to Tiam1. Such binding could explain the delay in axon elongation in MAP1B−/− neurons as a consequence of decreased activity of the Rho GTPases Rac1 and cdc42. Fluorescence microscopy using anti-MAP1B and anti-Tiam1 showed that Tiam1 and MAP1B colocalized mainly in axons of developing neurons (Figure 8, A–D). These results were confirmed in coimmunoprecipitation assays, in which an antiserum to MAP1B, but not the preimmune serum, was capable of coimmunoprecipitating Tiam1. Furthermore, reciprocal coimmunoprecipitation showed that an antiserum to Tiam1 was capable of

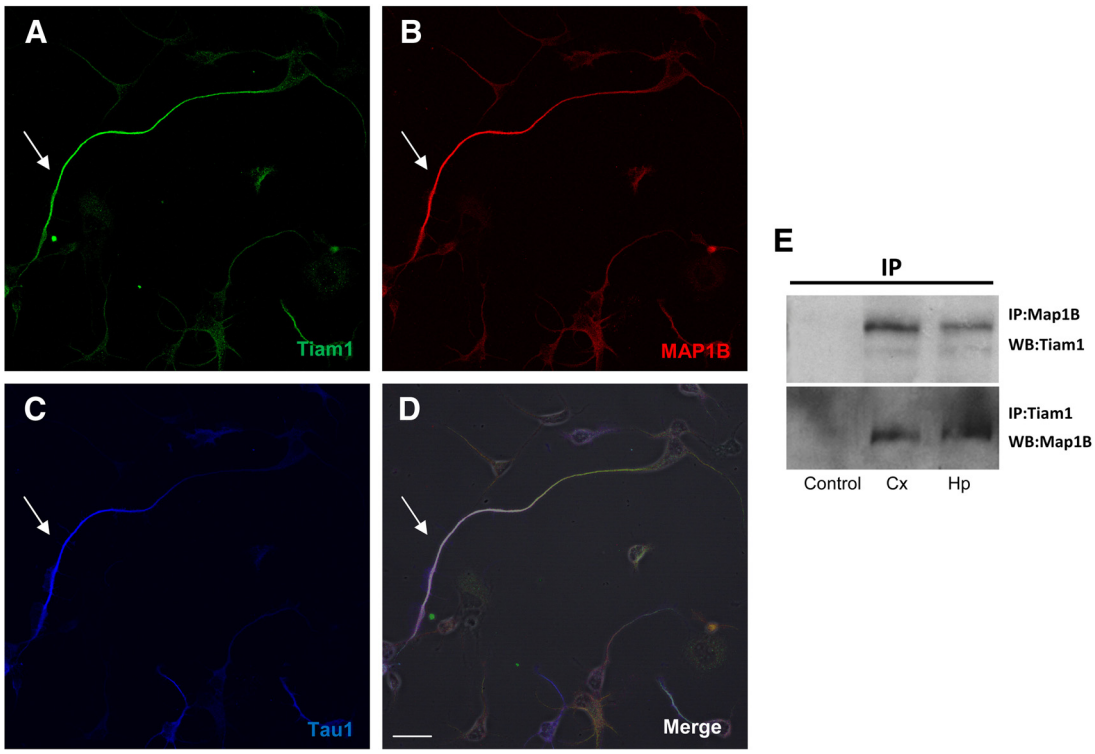

Figure 8. Tiam1 interacts with MAP1B. (A–D) Confocal images from a WT MAP1B neuron stained for Tiam1 (green, A), MAP1B (red, B), or Tau1 (blue, C). (D) A merge of images in A–C. Note that this protein colocalized mainly in the axon (arrow in each panel). Bar in D, 10 μm. (E) Coimmunoprecipitation (IP) of Tiam1 and MAP1B from brain extracts obtained from embryonic mouse cortex (Cx) and hippocampus (Hp). Antibodies against Tiam1 or MAP1B were used to visualize these proteins in Western blots (WB).

coimmunoprecipitating MAP1B (Figure 8E). These results suggest that MAP1B binds to Tiam1 and plays a role in regulating Rac1, which is required to induce axonal elongation.

DISCUSSION

Reorganization of the growth cone cytoskeleton involves lamellipodial expansion and protrusion, Rac1/cdc42 activation, and microtubule growth and invasion. This reorganization is essential for axon formation (Bradke and Dotti, 1999; Kunda *et al.*, 2001). It has been shown that localized activation of Rac1-GTPase contributes to the rapid elongation of the nascent axon (Kunda *et al.*, 2001). In this context, it has been reported that the Par3/Par6 complex of polarity may activate Rac1 by recruiting Tiam1, a Rac1-specific GEF. This recruitment may also depend on cdc42 activation (Nishimura *et al.*, 2005). Interestingly, signaling molecules located downstream of cdc42/Rac1 are also implicated in axonal elongation. Thus, neurons derived from cdc42-null mutant mice display decreased axonal elongation (Garvalov *et al.*, 2007). In this genetic model, cofilin phosphorylation levels are also altered (Garvalov *et al.*, 2007).

Here we present evidence that the microtubule-associated protein MAP1B participate in the regulation of the cross-talk between microtubules and actin microfilaments to promote axonal elongation. Our evidence shows that MAP1B deficiency produced a decrease in the activitys of the Rho-GTPases Rac1/cdc42 and an increase in RhoA activity. These results support many studies that indicate that members of the Rho family of small GTPases, including Rho, Rac1, and cdc42, seem to be the major players in regulating the cross-talk between actin and microtubules in developing neurons, for axon specification, guidance and elongation (Wittmann and Waterman-Storer, 2001). Moreover, during cell polarization, there is evidence of cross-talk between actin and microtubules via the small GTPase Rho. For example, IQGAP1, an effector of Rac1 and cdc42, interacts with CLIP-170, a protein that binds to the growing ends of microtubules (Fukata et al., 2002). PAK, another effector of Rac1 and cdc42, phosphorylates stathmin, which binds to microtubules and is able to destabilize them (Daub et al., 2001; Wittmann *et al.*, 2004). mDia is another protein that is implicated in this cross-talk between microtubules and actin, via Rho (Kodama *et al.*, 2003). Together these data indicate

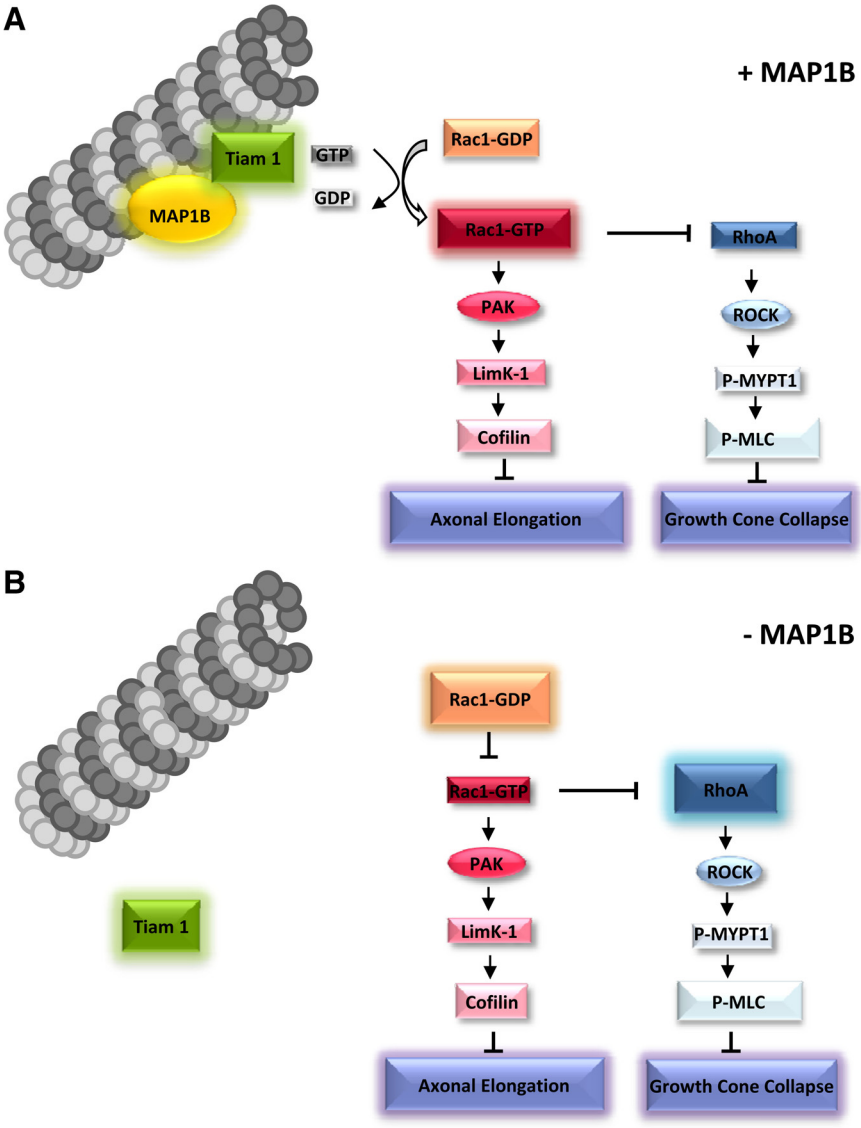

Figure 9. Schematic illustrating a potential mechanism to explain why MAP1B is necessary for Tiam1 activity. In the presence of MAP1B, Tiam1 is able to bind to microtubules. This binding appears to be required for efficient activation of cdc42 and Rac1. Activation of the Rac1 pathway results in the inhibition of cofilin, which permits actin polymerization and subsequent axon development. Moreover, Rac1 inhibits the RhoA pathway, thereby avoiding growth cone collapse. In the absence of MAP1B, Tiam1 is localized in the cytoplasm and does not activate the Rac1 pathway. Inhibition of the Rac1 pathway leads to activation of the RhoA pathway and growth cone collapse.

that several effectors of Rac1 and cdc42, including MAP1B, play a role in regulating cross-talk between actin and microtubules during axonal elongation.

Our results provide evidence that MAP1B-containing microtubules act as regulators of Rac1 activity during axon outgrowth through interactions with Tiam1 (Figure 9). Our results clearly indicate that MAP1B serves as a "flag" to target Tiam1 to a particular microtubule subset (e.g., Tyr-containing microtubules; Kunda *et al.*, 2001). This targeting contributes to the spatiotemporal activation of Rac1. Rac1 activation may not be only dependent on Tiam1 function, because it had been reported other GEFs contributing to neuronal polarity. Among them is DOCK7, which regulates neuronal polarity, and contribute to regulate the local phosphorylation of Stathmin/Op18 (Watabe-Uchida *et al.*, 2006). It follows, we cannot rule out the participation of this and other GEFs in our model. However in this work we focused on the study of Tiam1 for several reasons: 1) Tiam1 is expressed at high levels in the developing brain; 2)There is a high degree of temporal correlation between its expression and the morphological development of the axon; 3) Tiam1 protein levels peak 24 h after plating just at the time in which axon formation begins; and 4) Immunofluorescence studies show that in stage 3 neurons Tiam1 preferentially localizes to axonal shafts and their growth cones and finally and the most relevant point is that Tiam1 associates with microtubules (Kunda *et al.*, 2001). This point makes it an attractive candidate to interact with an MAP, such as MAP1B. Importantly, our data are consistent with previous reports that indicate an interaction between STEF (a homolog of Tiam1) and a subunit of MAP1B (Takefuji *et al.*, 2007). Interestingly, the STEF1-LC1 interaction is inhibited due to Rho-kinase–dependent phosphorylation of STEF1. In our study, Rho-kinase was activated in MAP1B-deficient cells, as indicated by our pulldown assays. Moreover, there was an increase in the phosphorylation of the myosin phosphatase target subunit 1 (MYPT1), the myosin-binding subunit of myosin phosphatase. Myosin phosphatase regulates the interaction of actin and myosin downstream of RhoA, which inhibits myosin phosphatase through the activation of Rho kinase. This inhibition would ultimately cause shrinkage of the axon and growth cone collapse. In addition, it has been shown that Rac1-dependent inhibition of RhoA signaling induces F-actin destabilization and promotes axonogenesis (Da Silva *et al.*, 2003; Sander *et al.*, 1999). Based on the results presented here and the literature, our model proposes that RhoA activation may depend on Rac1 inactivation. This model would explain the delay in axon outgrowth and the reduced rate of axonal elongation in MAP1B-deficient neurons. Additionally, the GEFs GEF-H1 and the Dbl-related protein, Lfc, which are specific for Rho and Rac1 interact with microtubules (Krendel *et al.*, 2002).

Interestingly, microtubules at the distal end of the axon, including the central and peripheral regions of the growth cone, were enriched in both MAP1B and Tiam1. In contrast, GTPase activation, as well as distal targeting of Tiam1, was absent in neurons lacking MAP1B. Thus, MAP1B deficiency was associated with increased Tiam1 localization in the cell body. The present observations raise the possibility that microtubules also regulate Rho-GTPase activity in developing neurons, similarly to such regulation in migrating fibroblasts.

On the other hand, it has been shown that MAP1B deficiency induces a dramatic decrease in the content of tyrosinated microtubules (Gonzalez-Billault *et al.*, 2001). Tubulin tyrosine ligase interacts with MAP1B in neuronal cells, suggesting that loss of this interaction may be in part responsible for decreased tyrosinated microtubules in MAP1B-deficient neurons (Utreras *et al.*, 2008). Posttranslational modifications of α-tubulin are needed for axon specification as indicated by studies showing increased acetylation of α-tubulin during axon initiation (Witte *et al.*, 2008). Moreover, these modifications (e.g., detyrosination of α-tubulin) also affected the binding of Tiam1 to microtubules.

In any case, the present observations raise the possibility that, in developing neurons, microtubules regulate Rho-GTPase activity, as proposed for migrating fibroblasts. Furthermore, regardless of the mechanism, the requirement of MAP1B for effective binding of Tiam1 to microtubules appears to define a new and crucial function for this MAP during neuronal polarization.

ACKNOWLEDGMENTS

This work was supported by FONDECYT (PICT 05-01697) and grants from FONCyT (PICT 815), Agencia Cordoba Ciencia, and HHMI to A.C. J.A. was supported by a Plan National Grant (SAF 2006-02424), CIBERNED and Comunidad de Madrid (SAL 0202-2006). C.G.-B. was supported by Fondecyt 1095089 and ICM P05-001-F.

REFERENCES

Arber, S., Barbayannis, F. A., Hanser, H., Schneider, C., Stanyon, C. A., Bernard, O., and Caroni, P. (1998). Regulation of actin dynamics through phosphorylation of cofilin by LIM-kinase. Nature *393*, 805–809.

Bamburg, J. R. (1999). Proteins of the ADF/cofilin family: essential regulators of actin dynamics. Annu. Rev. Cell Dev. Biol. *15*, 185–230.

Bamburg, J. R., and Bray, D. (1987). Distribution and cellular localization of actin depolymerizing factor. J. Cell Biol. *105*, 2817–2825.

Bishop, A. L., and Hall, A. (2000). Rho GTPases and their effector proteins. Biochem. J. *348*(Pt 2), 241–255.

Black, M. M., Slaughter, T., and Fischer, I. (1994). Microtubule-associated protein 1b (MAP1b) is concentrated in the distal region of growing axons. J. Neurosci. *14*, 857–870.

Bradke, F., and Dotti, C. G. (1997). Neuronal polarity: vectorial cytoplasmic flow precedes axon formation. Neuron *19*, 1175–1186.

Bradke, F., and Dotti, C. G. (1999). The role of local actin instability in axon formation. Science *283*, 1931–1934.

Cueille, N., Blanc, C. T., Popa-Nita, S., Kasas, S., Catsicas, S., Dietler, G., and Riederer, B. M. (2007). Characterization of MAP1B heavy chain interaction with actin. Brain Res. Bull. *71*, 610–618.

Da Silva, J. S., Medina, M., Zuliani, C., Di Nardo, A., Witke, W., and Dotti, C. G. (2003). RhoA/ROCK regulation of neuritogenesis via profilin IIa-mediated control of actin stability. J. Cell Biol. *162*, 1267–1279.

Daub, H., Gevaert, K., Vandekerckhove, J., Sobel, A., Hall, A. (2001). Rac/cdc42 and p65PAK regulate the microtubule-destabilizing protein stathmin through phosphorylation at serine 16. J. Biol. Chem. *276*, 1677–1680.

Del Rio, J. A., *et al.* (2004). MAP1B is required for Netrin 1 signaling in neuronal migration and axonal guidance. Curr. Biol. *14*, 840–850.

DiTella, M. C., Feiguin, F., Carri, N., Kosik, K. S., and Caceres, A. (1996). MAP-1B/TAU functional redundancy during laminin-enhanced axonal growth. J. Cell Sci. *109*(Pt 2), 467–477.

Edelmann, W., Zervas, M., Costello, P., Roback, L., Fischer, I., Hammarback, J. A., Cowan, N., Davies, P., Wainer, B., and Kucherlapati, R. (1996). Neuronal abnormalities in microtubule-associated protein 1B mutant mice. Proc. Natl. Acad. Sci. USA *93*, 1270–1275.

Fukata, M., Watanabe T., Noritake J., Nakagawa M., Yamaga M., Kuroda S., Matsuura Y., Iwamatsu A., Perez F., and Kaibuchi K. (2002) Rac1 and Cdc42 capture microtubules through IQGAP1 and CLIP-170. Cell *109*, 873–885.

Garvalov, B. K., Flynn, K. C., Neukirchen, D., Meyn, L., Teusch, N., Wu, X., Brakebusch, C., Bamburg, J. R., and Bradke, F. (2007). Cdc42 regulates cofilin during the establishment of neuronal polarity. J. Neurosci. *27*, 13117–13129.

Gonzalez-Billault, C., Avila, J., and Caceres, A. (2001). Evidence for the role of MAP1B in axon formation. Mol. Biol. Cell *12*, 2087–2098.

Gonzalez-Billault, C., *et al.* (2005). A role of MAP1B in Reelin-dependent neuronal migration. Cereb. Cortex *15*, 1134–1145.

Gonzalez-Billault, C., Demandt, E., Wandosell, F., Torres, M., Bonaldo, P., Stoykova, A., Chowdhury, K., Gruss, P., Avila, J., and Sanchez, M. P. (2000). Perinatal lethality of microtubule-associated protein 1B-deficient mice expressing alternative isoforms of the protein at low levels. Mol. Cell Neurosci. *16*, 408–421.

Ik-Tsen Heng, J., Chariot, A., and Nguyen, L. (2009). Molecular layers underlying cytoskeletal remodelling during cortical development. Cell Press *33*(1), 38–47.

Inagaki, N., Chihara, K., Arimura, N., Menager, C., Kawano, Y., Matsuo, N., Nishimura, T., Amano, M., and Kaibuchi, K. (2001). CRMP-2 induces axons in cultured hippocampal neurons. Nat. Neurosci. *4*, 781–782.

Kodama, A., Karakesisoglou, I., Wong, E., Vaezi, A., and Fuchs, E. (2003). ACF7, an essential integrator of microtubule dynamics. Cell *115*, 343–354.

Krendel, M., Zenke, F. T., and Bokoch, G. M. (2002). Nucleotide exchange factor GEF-H1 mediates cross-talk between microtubules and the actin cytoskeleton. Nat. Cell Biol. *4*, 294–301.

Kunda, P., Paglini, G., Quiroga, S., Kosik, K., and Caceres, A. (2001). Evidence for the involvement of Tiam1 in axon formation. J. Neurosci. *21*, 2361–2372.

Luo, L. (2000). Rho GTPases in neuronal morphogenesis. Nat. Rev. Neurosci. *1*, 173–180.

Luo, L. (2002). Actin cytoskeleton regulation in neuronal morphogenesis and structural plasticity. Annu. Rev. Cell Dev. Biol. *18*, 601–635.

Maekawa, M., Ishizaki, T., Boku, S., Watanabe, N., Fujita, A., Iwamatsu, A., Obinata, T., Ohashi, K., Mizuno, K., and Narumiya, S. (1999). Signaling from Rho to the actin cytoskeleton through protein kinases ROCK and LIM-kinase. Science *285*, 895–898.

Meixner, A., Haverkamp, S., Wassle, H., Fuhrer, S., Thalhammer, J., Kropf, N., Bittner, R. E., Lassmann, H., Wiche, G., and Propst, F. (2000). MAP1B is required for axon guidance and Is involved in the development of the central and peripheral nervous system. J. Cell Biol. *151*, 1169–1178.

Nakata, T., and Hirokawa, N. (1987). Cytoskeletal reorganization of human platelets after stimulation revealed by the quick-freeze deep-etch technique. J. Cell Biol. *105*, 1771–1780.

Ng, J., Nardine, T., Harms, M., Tzu, J., Goldstein, A., Sun, Y., Dietzl, G., Dickson, B. J., and Luo, L. (2002). Rac GTPases control axon growth, guidance and branching. Nature *416*, 442–447.

Nishimura, T., Yamaguchi, T., Kato, K., Yoshizawa, M., Nabeshima, Y., Ohno, S., Hoshino, M., and Kaibuchi, K. (2005). PAR-6-PAR-3 mediates Cdc42-induced Rac activation through the Rac GEFs STEF/Tiam1. Nat. Cell Biol. *7*, 270–277.

Paglini, G., Kunda, P., Quiroga, S., Kosik, K., and Caceres, A. (1998). Suppression of radixin and moesin alters growth cone morphology, motility, and process formation in primary cultured neurons. J. Cell Biol. *143*, 443–455.

Pedrotti, B., and Islam, K. (1996). Dephosphorylated but not phosphorylated microtubule associated protein MAP1B binds to microfilaments. FEBS Lett. *388*, 131–133.

Riederer, B. M. (2007). Microtubule-associated protein 1B, a growth-associated and phosphorylated scaffold protein. Brain Res. Bull. *71*, 541–558.

Ruthel, G., and Banker, G. (1999). Role of moving growth cone-like "wave" structures in the outgrowth of cultured hippocampal axons and dendrites. J. Neurobiol. *39*, 97–106.

Ruthel, G., and Hollenbeck, P. J. (2000). Growth cones are not required for initial establishment of polarity or differential axon branch growth in cultured hippocampal neurons. J. Neurosci. *20*, 2266–2274.

Sander, E. E., ten Kooster, J. P., van Delft, S., van der Kammen, R. A., and Collard, J. G. (1999). Rac downregulates Rho activity: reciprocal balance between both GTPases determines cellular morphology and migratory behavior. J. Cell Biol. *5*, 1009–1022.

Sarmiere, P. D., and Bamburg, J. R. (2004). Regulation of the neuronal actin cytoskeleton by ADF/cofilin. J. Neurobiol. *58*, 103–117.

Sosa, L., Dupraz, S., Laurino, L., Bollati, F., Bisbal, M., Caceres, A., Pfenninger, K. H., and Quiroga, S. (2006). IGF-1 receptor is essential for the establishment of hippocampal neuronal polarity. Nat. Neurosci. *9*, 993–995.

Takefuji, M., *et al.* (2007). Rho-kinase modulates the function of STEF, a Rac GEF, through its phosphorylation. Biochem. Biophys. Res. Commun. *355*, 788–794.

Takei, Y., Kondo, S., Harada, A., Inomata, S., Noda, T., and Hirokawa, N. (1997). Delayed development of nervous system in mice homozygous for disrupted microtubule-associated protein 1B (MAP1B) gene. J. Cell Biol. *137*, 1615–1626.

Takei, Y., Teng, J., Harada, A., and Hirokawa, N. (2000). Defects in axonal elongation and neuronal migration in mice with disrupted tau and map1b genes. J. Cell Biol. *150*, 989–1000.

Utreras, E., Jimenez-Mateos, E. M., Contreras-Vallejos, E., Tortosa, E., Perez, M., Rojas, S., Saragoni, L., Maccioni, R. B., Avila, J., and Gonzalez-Billault, C. (2008). Microtubule-associated protein 1B interaction with tubulin tyrosine ligase contributes to the control of microtubule tyrosination. Dev. Neurosci. *30*, 200–210.

Watabe-Uchida, M., Keisha, J., Janas Justyna, A., Newey, S. E., and Van Aelst, L. (2006). The Rac activator Dock7 regulates neuronal polarity through local phosphorylatin of stathmin/Op18. Neuron *51*, 727–739.

Waterman-Storer, C. M., Worthylake, R. A., Liu, B. P., Burridge, K., and Salmon, E. D. (1999). Microtubule growth activates Rac1 to promote lamellipodial protrusion in fibroblasts. Nat. Cell Biol. *1*, 45–50.

Witte, H., Neukirchen, D., and Bradke, F. (2008). Microtubule stabilization specifies initial neuronal polarization. J. Cell Biol. *180*, 619–632.

Wittmann, T., and Waterman-Storer, C. M. (2001). Cell motility: can Rho GTPases and microtubules point the way? J. Cell Sci. *114*, 3795–3803.

Wittmann, T., Bokoch, G. M., and Waterman-Storer, C. M. (2004). Regulation of microtubule destabilizing activity of Op18/stathmin downstream of Rac1. J. Biol. Chem. *279*(7), 6196–6203.

Yang, N., Higuchi, O., Ohashi, K., Nagata, K., Wada, A., Kangawa, K., Nishida, E., and Mizuno, K. (1998). Cofilin phosphorylation by LIM-kinase 1 and its role in Rac-mediated actin reorganization. Nature *393*, 809–812.